Sensor and Simulation Notes

Note 139

October 1971

A Vertical Post Inside a Two-Parallel-Plate Simulator

by

K. S. H. Lee
Northrop Corporate Laboratories
Pasadena, California

Abstract

The problem at hand is to examine how the electromagnetic response of a cylindrical post changes inside a two-parallel-plate simulator as the post is moved vertically up and down between the two plates. The frequency and time variations of the induced total current and charges on both ends of the post are plotted with the post's position inside the simulator as a parameter. The field enhancement factors at the post's ends and the decay time of the lowest order mode of the current are graphed as well as tabulated against the post's position inside the simulator.

I. Introduction

In SSN 111 we have studied the electromagnetic behavior of a cylindrical post resting vertically on the ground plane of a two-parallel-plate simulator. When the post rises too high and almost touches the top plate of the simulator, the scattered electric field near the top end of the post will become intolerably large and air breakdown may result. One way to inhibit such a large field is to make a hole in the top plate, and the results of making such a hole have been reported in SSN 121. These two problems can, from the image theory, be viewed as the electromagnetic interaction problem of a vertical post symmetrically placed inside a two-parallel-plate simulator.

A natural extension of the above symmetric case is the one where the vertical post is unsymmetrically located in the simulator, as shown in Fig. 1. When the post is close to the bottom plate but far away from the top plate, one may consider the interaction problem of a vertical post above a ground plane. This problem has many other applications and is important enough to be treated in its own right. Accordingly, this problem has been studied in sufficient detail in SSN 134 and SSN 136. In the present note we report the results of the problem depicted in Fig. 1. Again, the quantities of importance are the post's resonant frequencies, the field enhancement factors at both ends of the post, the frequency variation and time history (for a step-function incident wave) of the post's total current together with the decay time of its lowest order mode. Our primary interest is how these quantities deviate from their symmetric values when the post is moved vertically up and down between the two plates.

The generalization of this and all previous studies is to consider the case where the post is arbitrarily oriented and located inside the two parallel plates. The study of this general problem is already underway.

In section II we present the necessary mathematical apparatus for computer programming. In section III we report the numerical results in graphical and/or tabular form.

II. Integral Equation for the Post's Total Current

Consider figure 1 where a time-harmonic plane wave of the form

$$\underline{H}^{inc} = - \underline{e}_y H_o e^{ikx}$$

strikes the post from the left. Here and henceforth, the time convention $e^{-i\omega t}$ is used. Following exactly the procedure that leads from equation (1) to equation (5) in reference 1, we have

$$\frac{1}{2} I(z) + \int_\Delta^{2h+\Delta} K(a,z';a,z)I(z')dz'$$

$$= - 2\pi i a H_o J_1(ka) + a \int_o^a d\rho' \left[I_1 \frac{\partial G}{\partial z'} \right]_{z'=2h+\Delta} - a \int_o^a d\rho' \left[I_2 \frac{\partial G}{\partial z'} \right]_{z'=\Delta} \quad (1)$$

where

$$I(z) = 2\pi a H_\phi(a,z)$$

$$I_1 \doteq I(2h + \Delta)[1 - (1 - \rho^2/a^2)^{2/3}] \quad (2)$$

$$I_2 \doteq I(\Delta)[1 - (1 - \rho^2/a^2)^{2/3}]$$

I_1 (I_2) is actually the total current flowing radially inward (outward) on the top (bottom) end of the post. In equation (1), K and G are given by[1]

$$K(\rho,z;a,z') = - \left[\frac{\partial}{\partial \rho'} (\rho'G) \right]_{\rho'=a}$$

$$G(\rho,z;\rho',z') = \int_o^{2\pi} d\phi \cos\phi \sum_{m=-\infty}^\infty \left\{ \frac{e^{ikR_m^{(+)}}}{4\pi R_m^{(+)}} + \frac{e^{ikR_m^{(-)}}}{4\pi R_m^{(-)}} \right\} \quad (3)$$

where

$$R_m^{(+)} = [(4ms + z + z')^2 + \rho^2 + \rho'^2 - 2\rho\rho' \cos\phi]^{\frac{1}{2}}$$

$$R_m^{(-)} = \left[(4ms - z + z')^2 + \rho^2 + \rho'^2 - 2\rho\rho' \cos \phi\right]^{\frac{1}{2}}$$

Equations (1) - (3) were programmed for numerical computation and the results will be reported in the next section.

III. Numerical Results

Figure 1 shows that apart from the wavelength $2\pi/k$ of the incident wave, there are 4 length parameters in the problem, namely, h, a, s, and Δ. If we normalize all the length parameters with respect to h, we are left with 3 dimensionless parameters a/h, s/h and Δ/h, putting aside the parameter kh (frequency domain) and the parameter ct/h (time domain). Since our object here is to study the deviations of some quantities from their values corresponding to the symmetric case where the vertical post is situated halfway between the two plates, we should let Δ/h vary over a wide range of values for fixed a/h and s/h. Then we are able to plot various quantities normalized with respect to their corresponding symmetric values against Δ/h with a/h and s/h as parameters. In the following we shall present extensive numerical results for one value of a/h and two values of s/h, namely,

$$a/h = 0.1 \qquad h/s = \begin{cases} 0.4 \\ 0.6 \end{cases}$$

For other values of a/h and h/s, one can get a fairly good feeling about what happens from the results of this note and those in SSN 111, where we have provided, for the symmetric case, extensive results for a wide range of values for h/s and two values of a/h.

The frequency variation and time history (for a step-function incident plane wave) of the total induced current are presented in Figs. 2a-3f. The superscript s on a quantity in Figs. 2f and 3f serves to remind us that that quantity is referred to the symmetric case. In Tables I and II below we give the normalized decay time as a function of Δ/h.

Figures 4a-4e and figures 5a-5e give the frequency variations (for a unit time-harmonic incident plane wave) and the time histories (for a step-function incident plane wave) of the total induced charges on the top and bottom ends of the post. In Figs. 4f and 5f we graph these quantities, $C_s/C_s^{(s)}$, $C_r/C_r^{(s)}$ and $C_m/C_m^{(s)}$, against Δ/h and we also tabulate them in Tables III and IV. For more precise definitions of these quantities the reader can refer to pages 22-23 of SSN 111.

5

Table I. Decay Time

$h/s = .4$ $a/h = .1$ $\tau^{(s)} = 5.825 \ h/c$

Δ/h	$\tau/\tau^{(s)}$
0	1.029
.2	.519
.4	.432
.6	.532
.8	.670
1.0	.809
1.2	.922
1.4	.993
1.5	1.000

Table II. Decay Time

$h/s = .6$ $a/h = .1$ $\tau^{(s)} = 2.740 \ h/c$

Δ/h	$\tau/\tau^{(s)}$
0	1.518
.2	1.200
.3	1.020
.4	1.037
.5	.990
.6	.967
2/3	1.000

Table III. Induced Charges on the Post's Ends

$$h/s = .4 \qquad a/h = .1$$
$$c_s^{(s)} = 6.250 \qquad c_r^{(s)} = 17.263 \qquad c_m^{(s)} = 9.575$$

	Bottom End			Top End		
Δ/h	$c_s/c_s^{(s)}$	$c_m/c_m^{(s)}$	$c_r/c_r^{(s)}$	$c_s/c_s^{(s)}$	$c_m/c_m^{(s)}$	$c_r/c_r^{(s)}$
0				1.623	1.052	.517
.2	1.200	1.012	.774	1.038	.963	.601
.4	1.070	.993	.744	1.014	.974	.687
.6	1.029	.989	.772	1.007	.991	.772
.8	1.011	.989	.828	1.002	.996	.858
1.0	1.005	.990	.890	1.001	.998	.933
1.2	1.003	.994	.950	1.000	.999	.980
1.4	1.001	.997	.988	1.000	1.000	.998
1.5	1.000	1.000	1.000	1.000	1.000	1.000

Table IV. Induced Charges on the Post's Ends

$$h/s = .6 \qquad a/h = .1$$
$$c_s^{(s)} = 6.481 \qquad c_r^{(s)} = 12.897 \qquad c_m^{(s)} = 9.728$$

	Bottom End			Top End		
Δ/h	$c_s/c_s^{(s)}$	$c_m/c_m^{(s)}$	$c_r/c_r^{(s)}$	$c_s/c_s^{(s)}$	$c_m/c_m^{(s)}$	$c_r/c_r^{(s)}$
0				1.600	1.053	.555
.2	1.167	1.020	1.111	1.012	.973	.800
.3	1.077	1.012	1.063	1.000	.985	.871
.4	1.033	1.006	1.040	1.000	.993	.920
.5	1.015	1.001	1.024	1.000	.998	.957
.6	1.005	1.000	1.009	1.000	1.000	.985
2/3	1.000	1.000	1.000	1.000	1.000	1.000
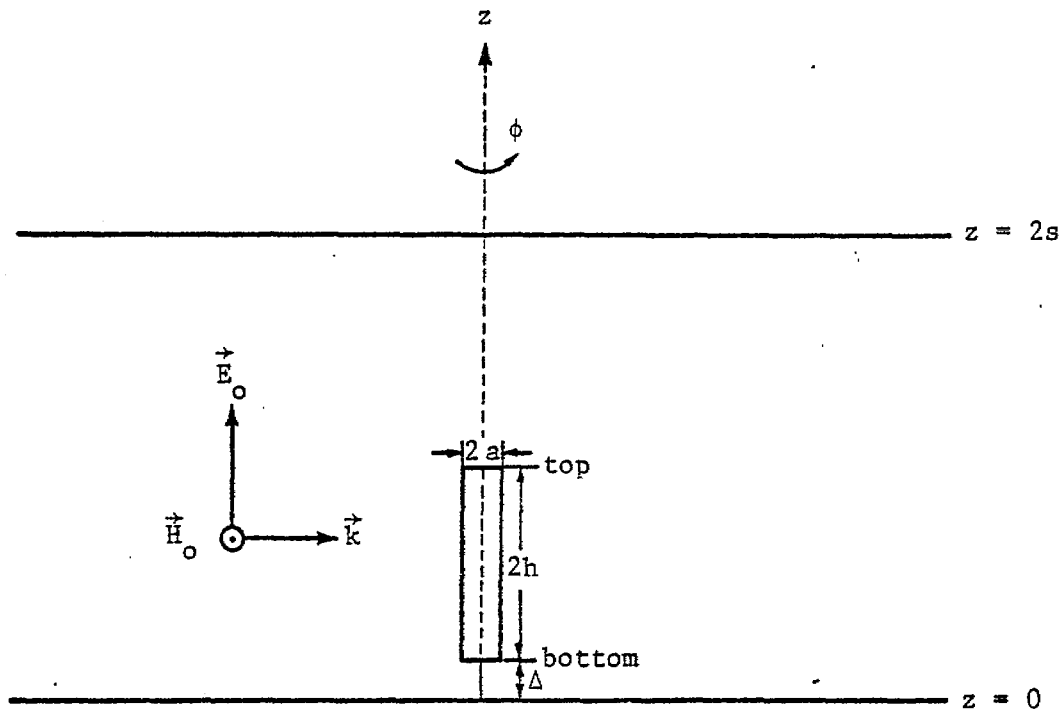
Figure 1. Side view of a cylindrical rod inside two parallel plates.
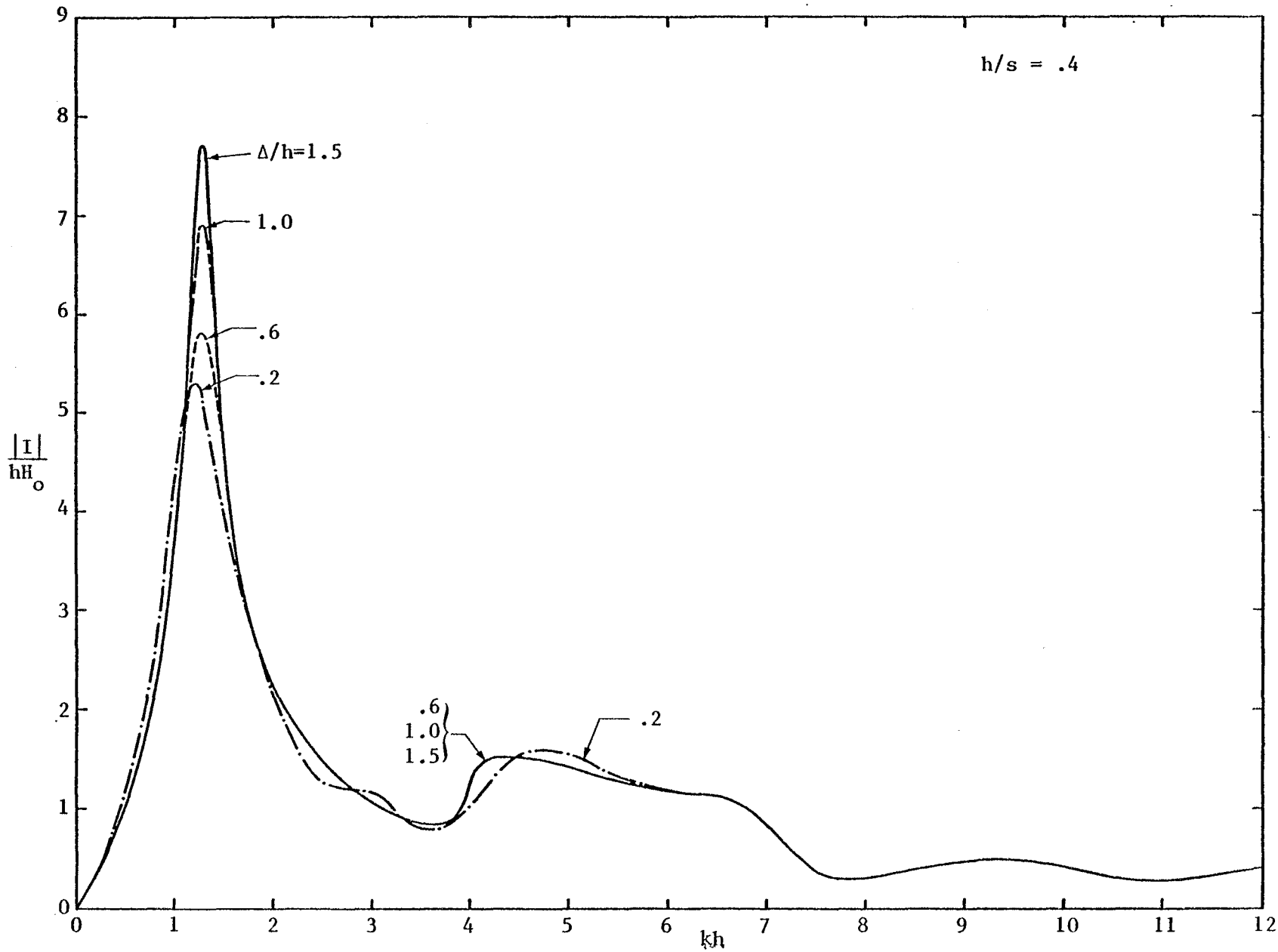
Figure 2a. Frequency variation of current at a distance of 1/4(post length) from the post's bottom end; i.e., at z = Δ + h/2 (see Fig. 1).

Figure 2b. Frequency variation of current at the post's mid-section.
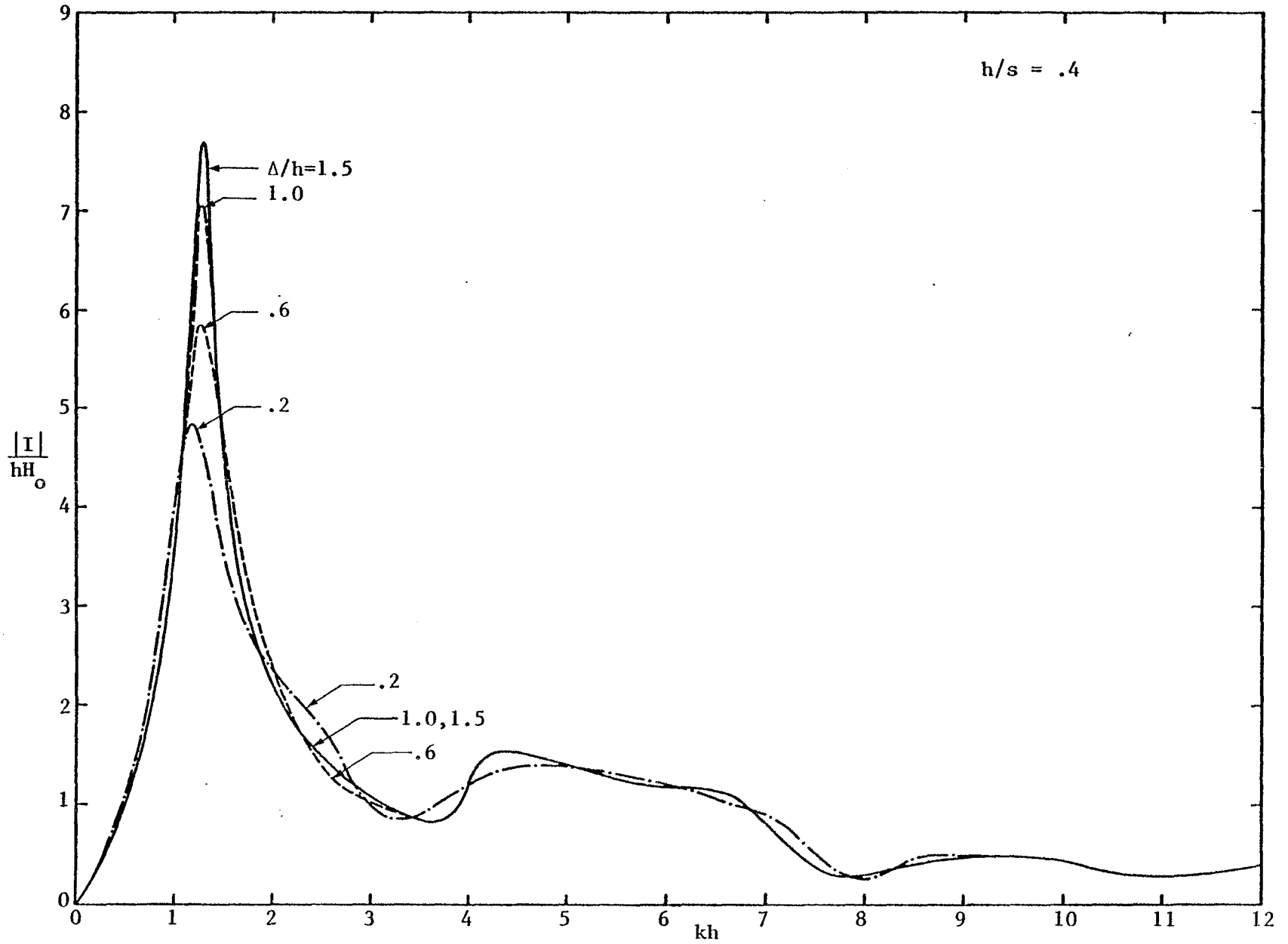
Figure 2c. Frequency variation of current at a distance of 3/4(post length) from the post's bottom end; i.e., at $z = \Delta + 3h/2$ (see Fig. 1).
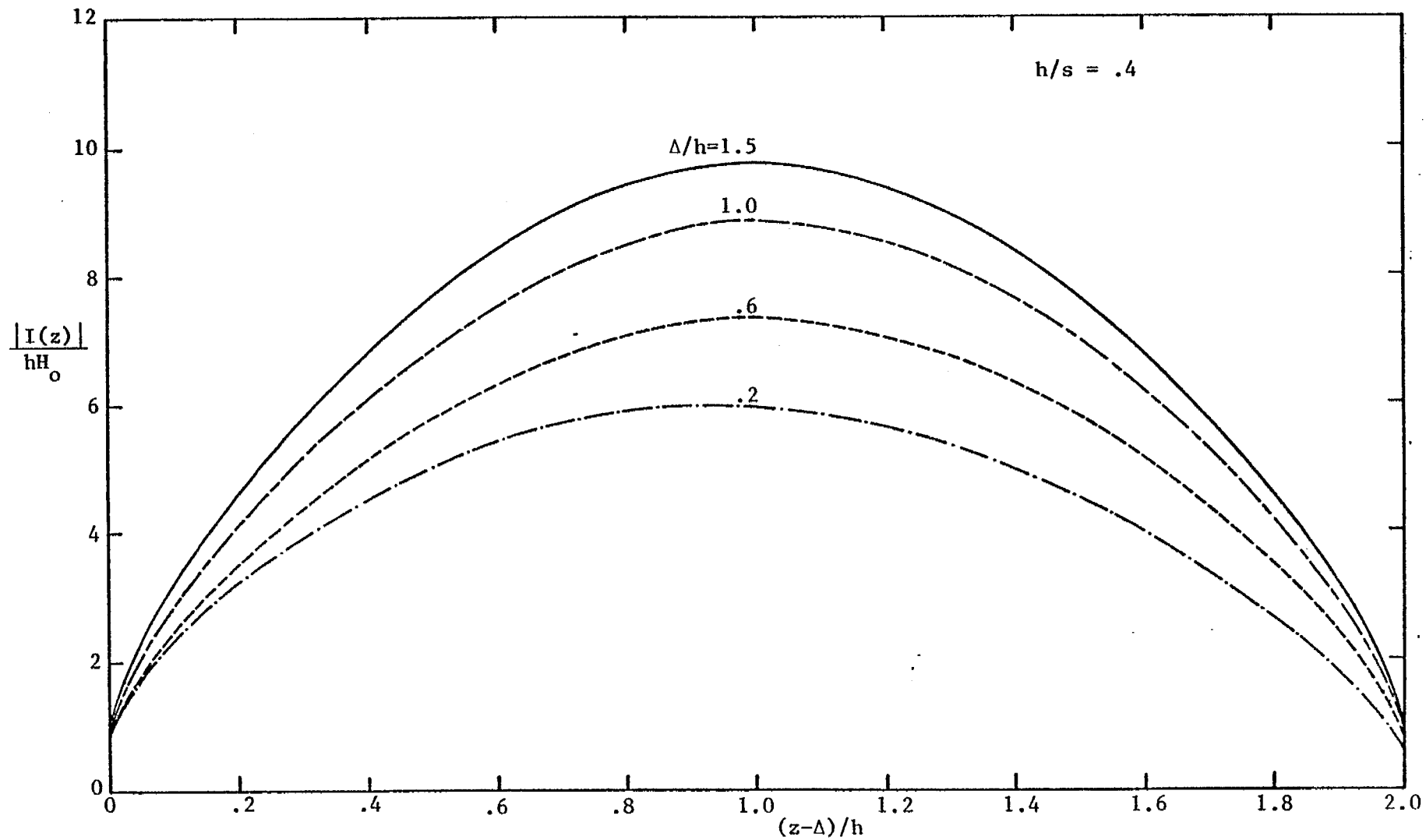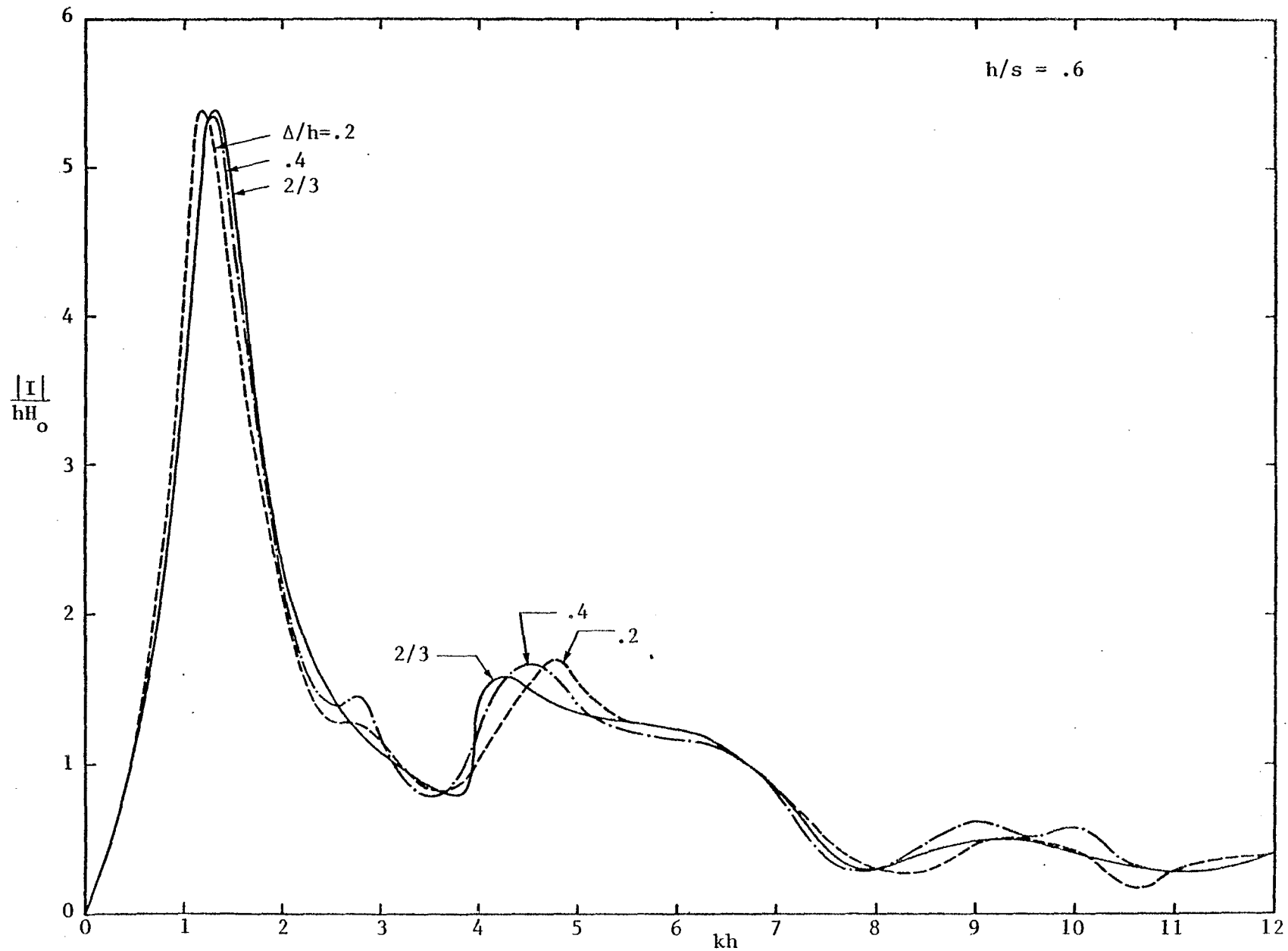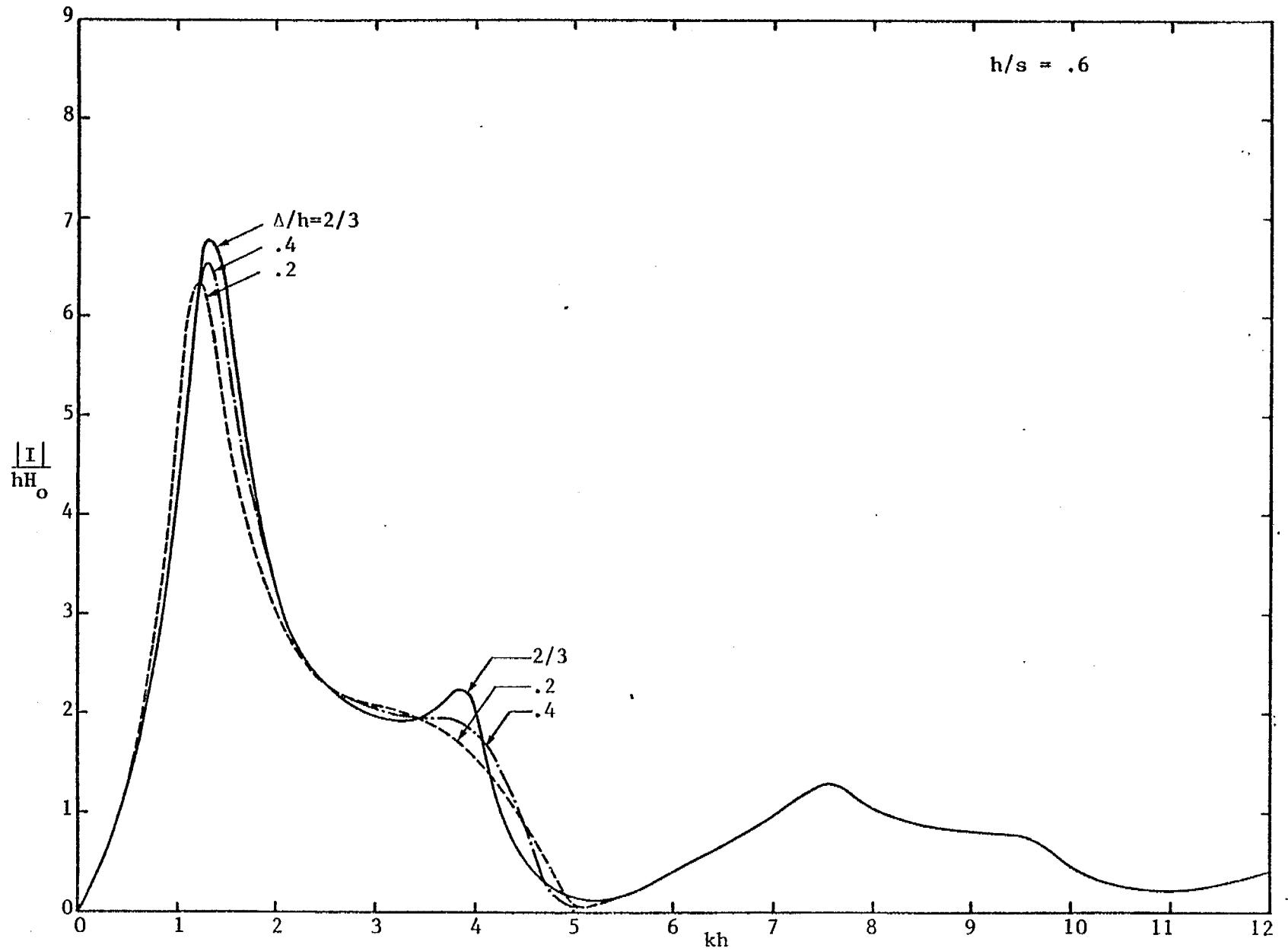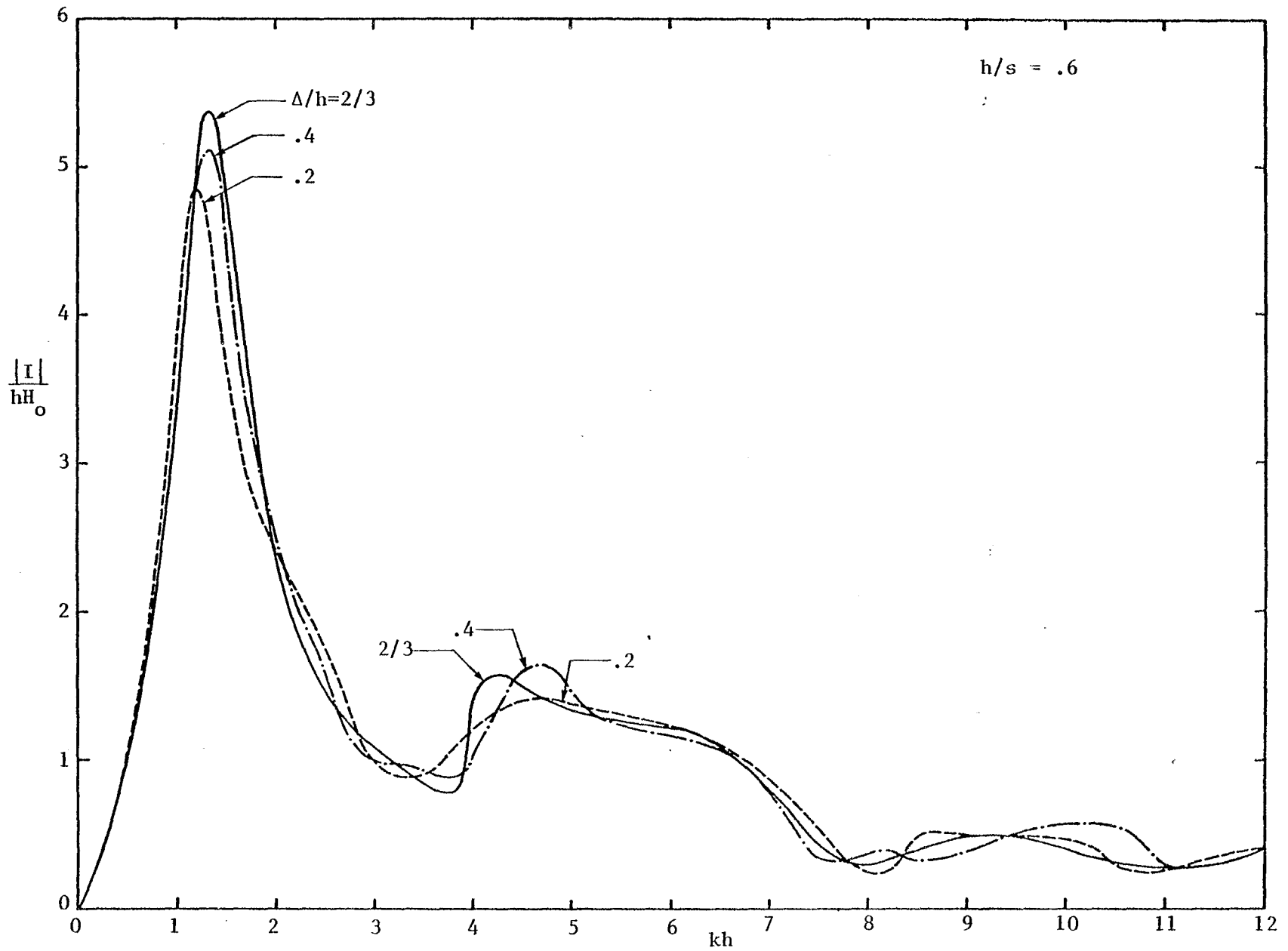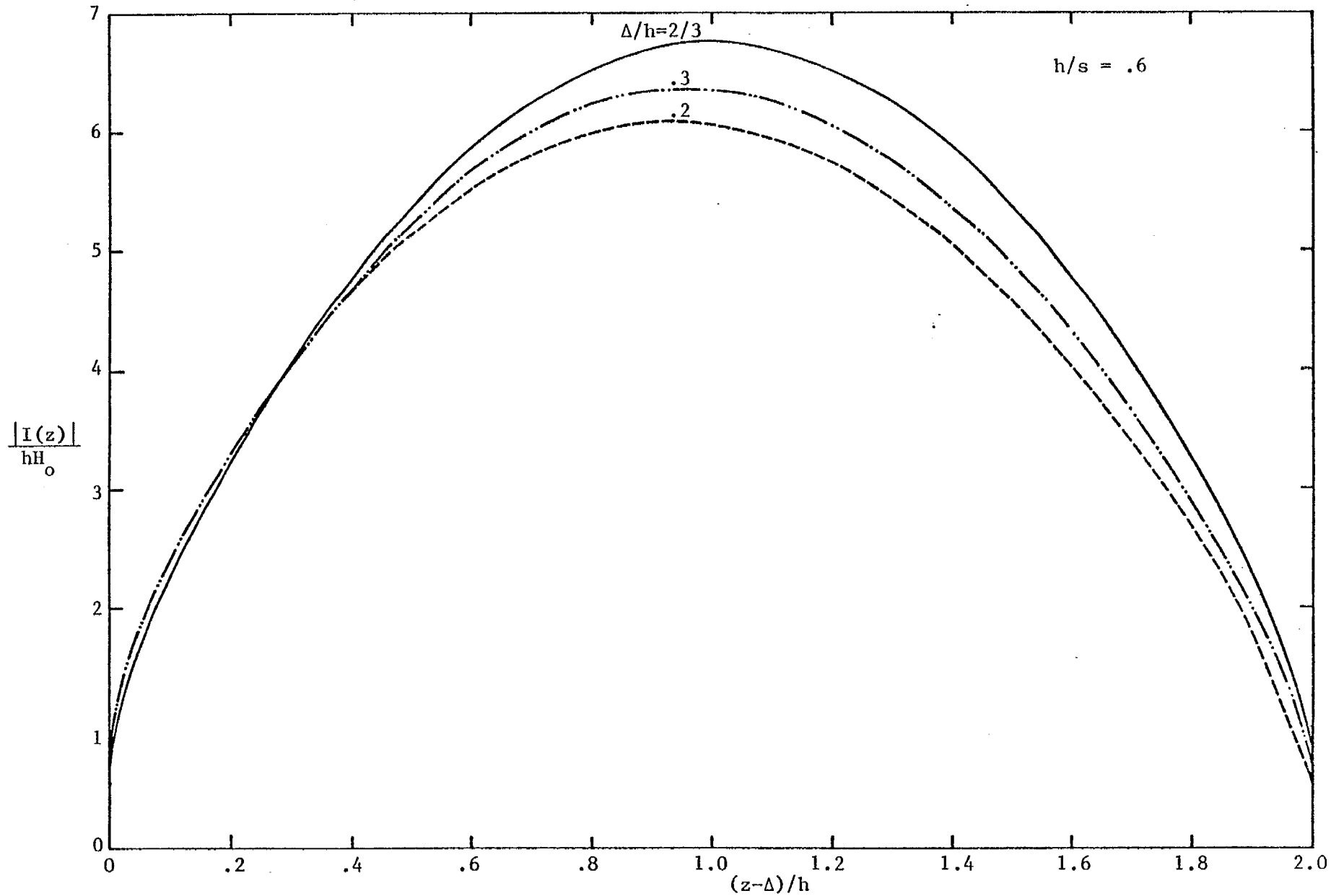
Figure 2d.   Post current versus position at kh=1.3 (free-space first resonant frequency k_oh=1.23).
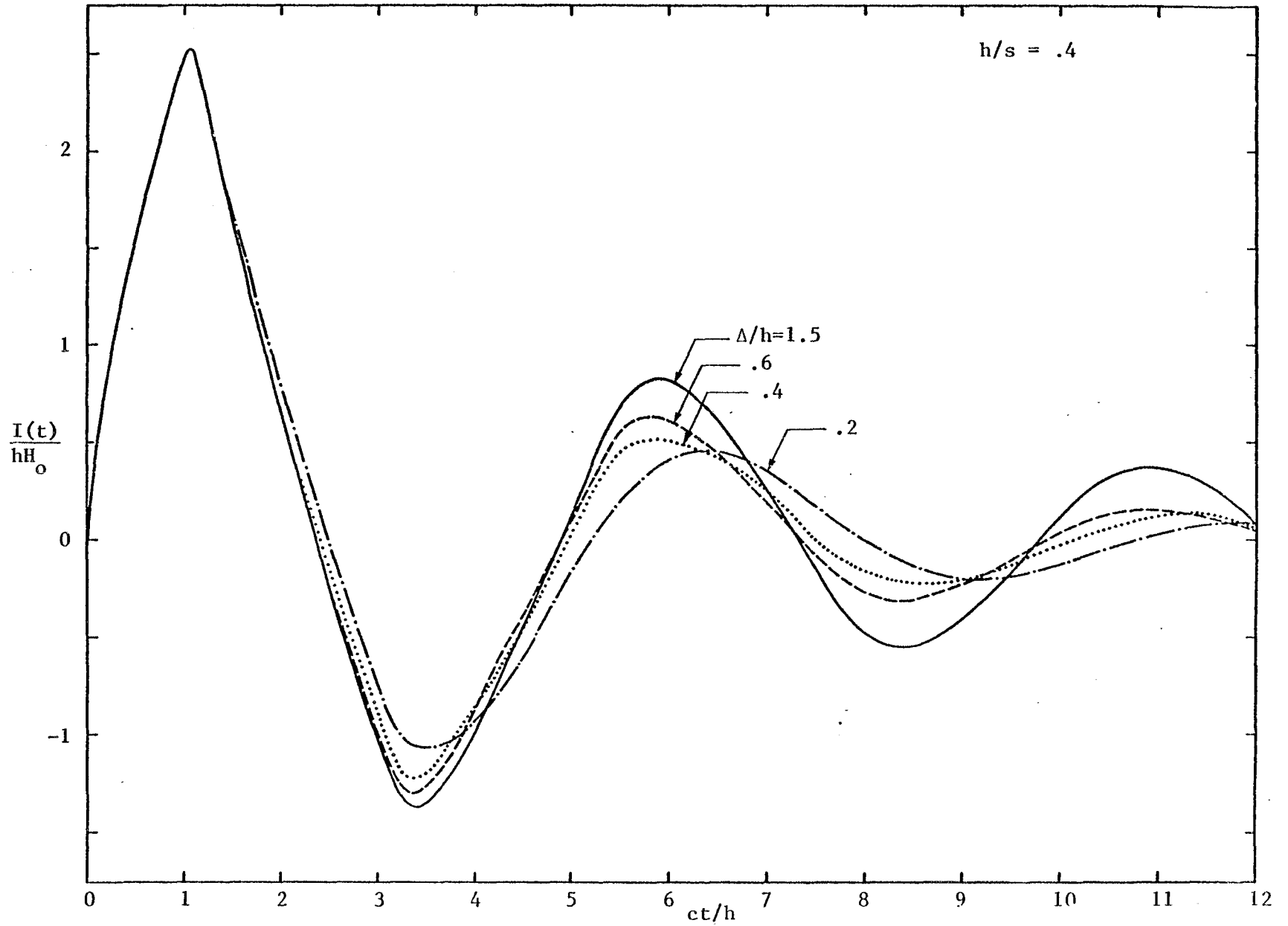
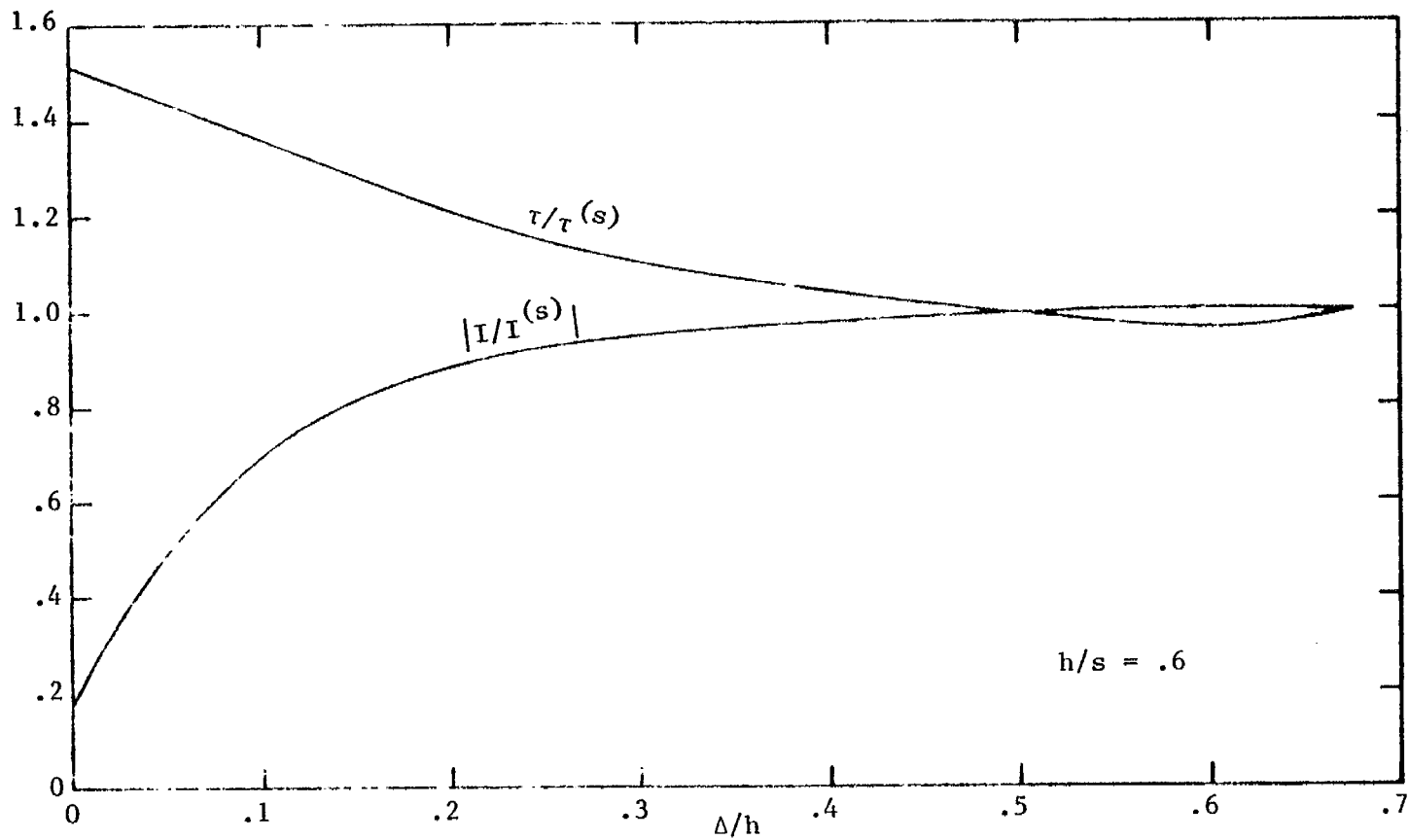Figure 2e. Time history of current at the post's mid-section.
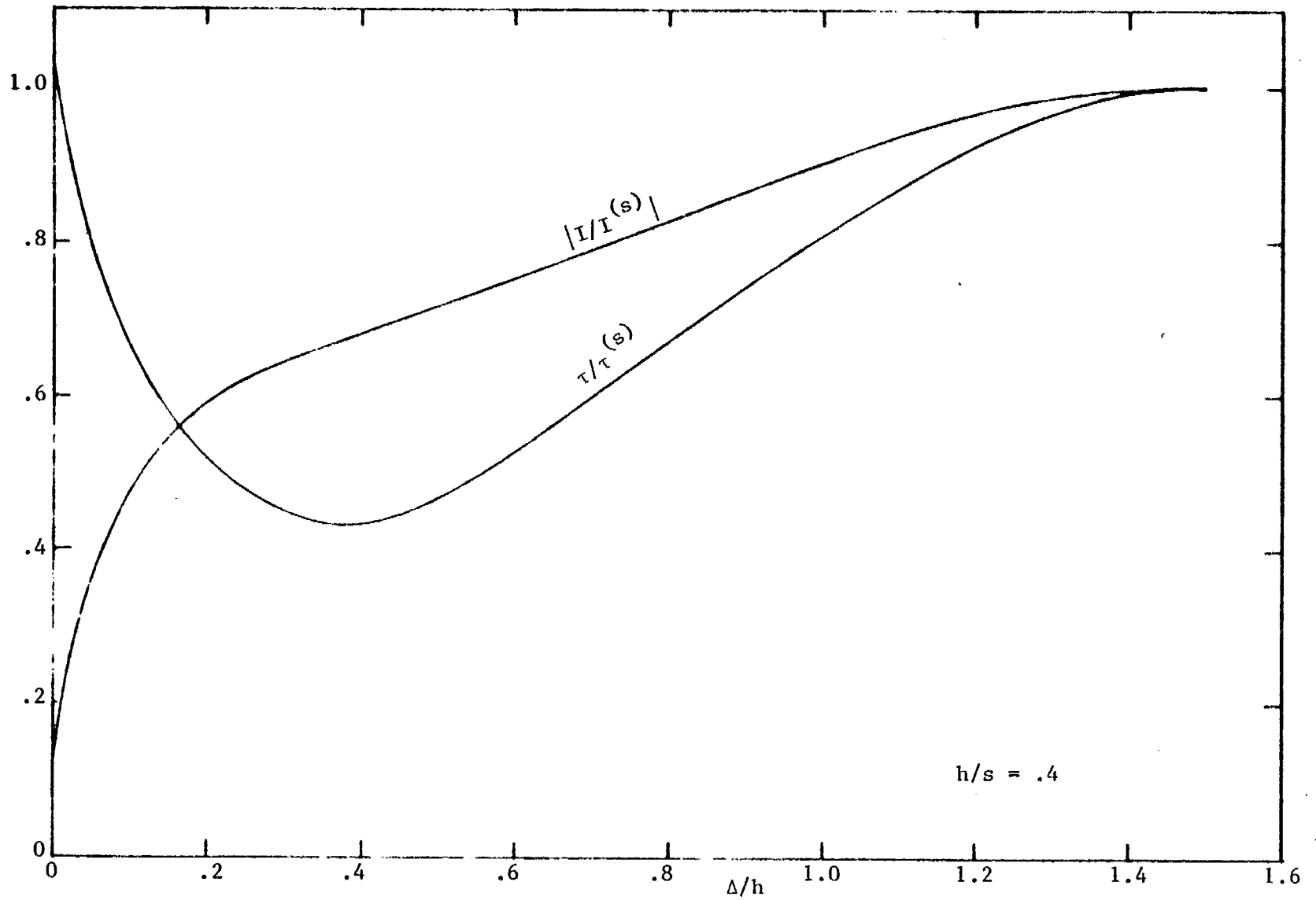
Figure 2f. Current $\left|I/I^{(s)}\right|$ induced at $z = \Delta + h$ by plane wave of frequency $\omega = 1.3\ c/h$ and the decay time $\tau/\tau^{(s)}$ of the fundamental mode versus Δ/h.

Figure 3a. Frequency variation of current at a distance of 1/4(post length) from the post's bottom end; i.e., at $z = \Delta + h/2$ (see Fig. 1).

Figure 3b. Frequency variation of current at the post's mid-section.

Figure 3c. Frequency variation of current at a distance of 3/4(post length) from the post's bottom end; i.e., at z = Δ + 3h/2 (see Fig. 1).

17

Figure 3d. Post current versus position at kh=1.3 (free-space first resonant frequency $k_o h$=1.23)
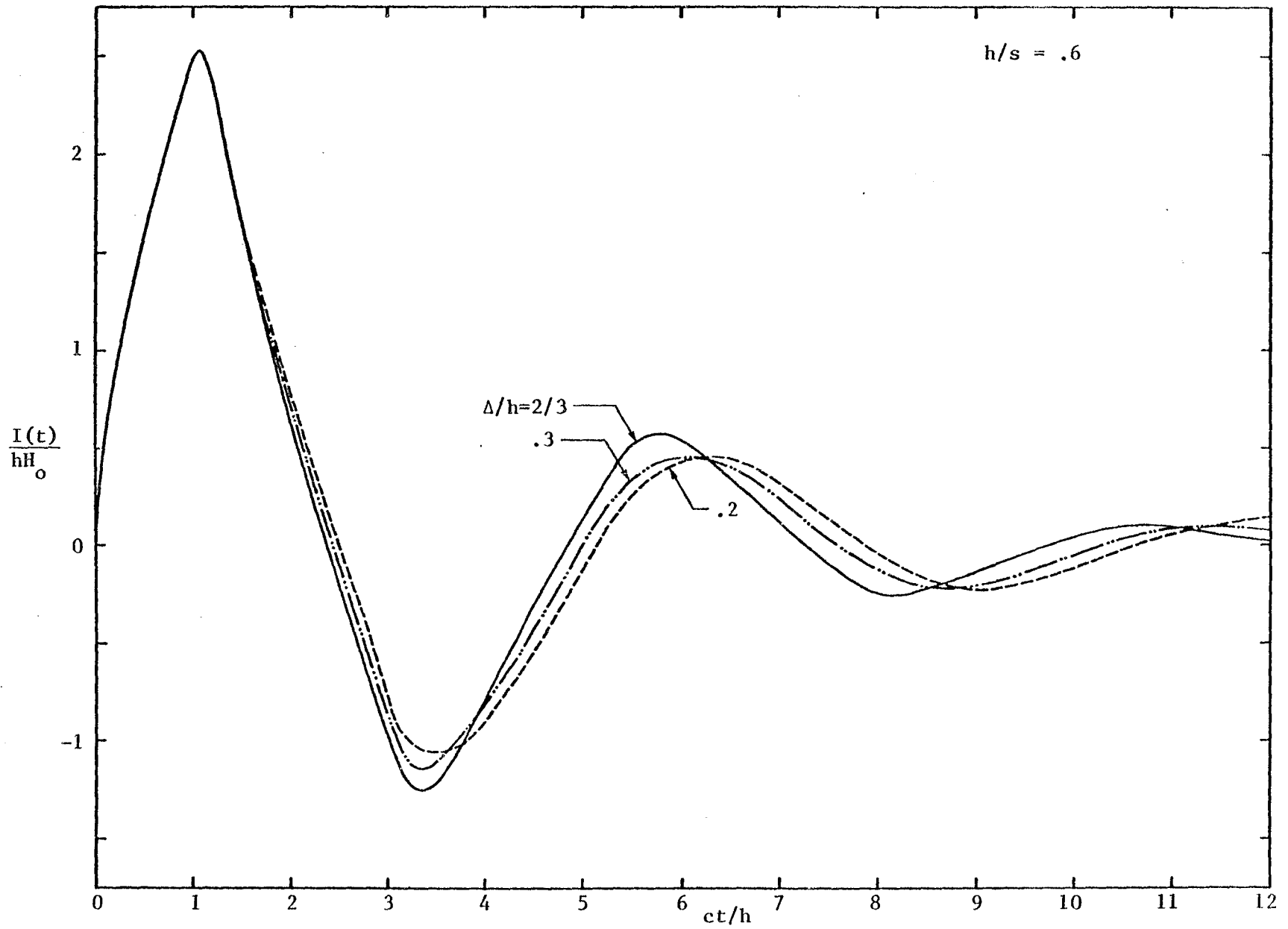
Figure 3e. Time history of current at the post's mid-section.

Figure 3f. Current $\left|I/I^{(s)}\right|$ induced at $z = \Delta + h$ by plane wave of frequency $\omega = 1.3$ c/h and the decay time $\tau/\tau^{(s)}$ of the fundamental mode versus Δ/h.
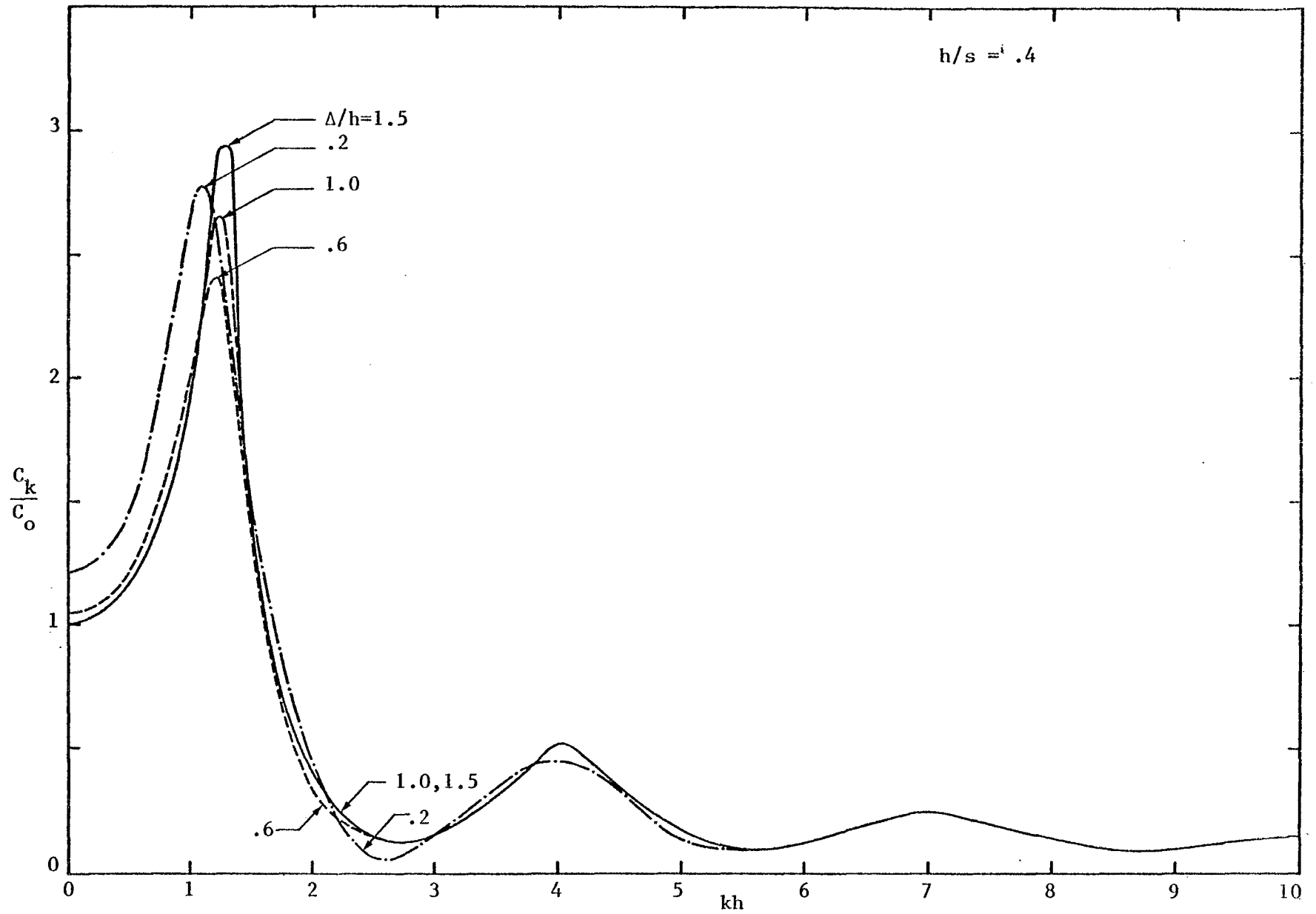
Figure 4a. Frequency variation of total surface charge density at the post's bottom end.
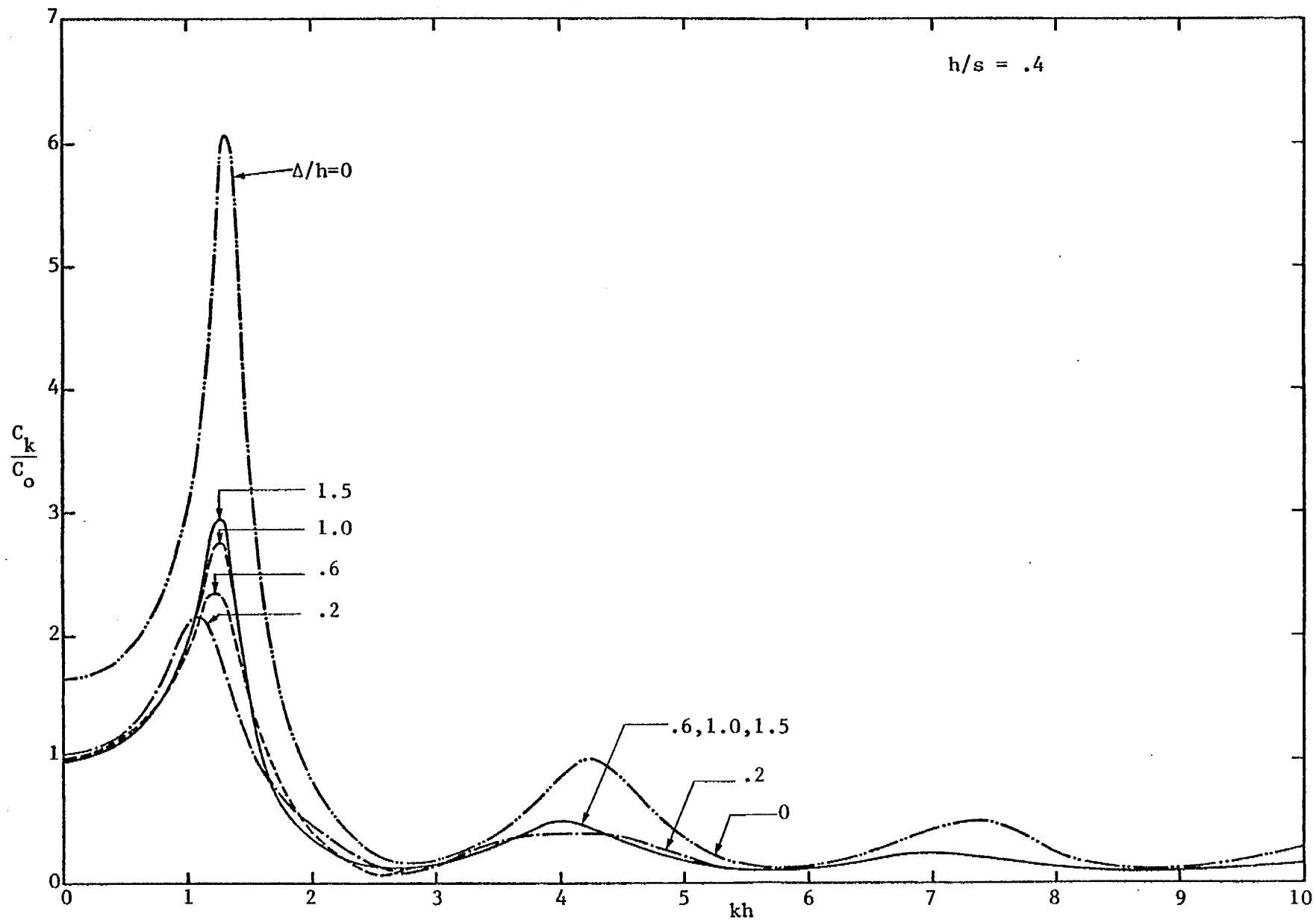
Figure 4b. Frequency variation of total surface charge density at the post's top end.

$$\frac{C(t)}{C_o}$$

h/s = .4

Δ/h=.2

.6

1.5

ct/h
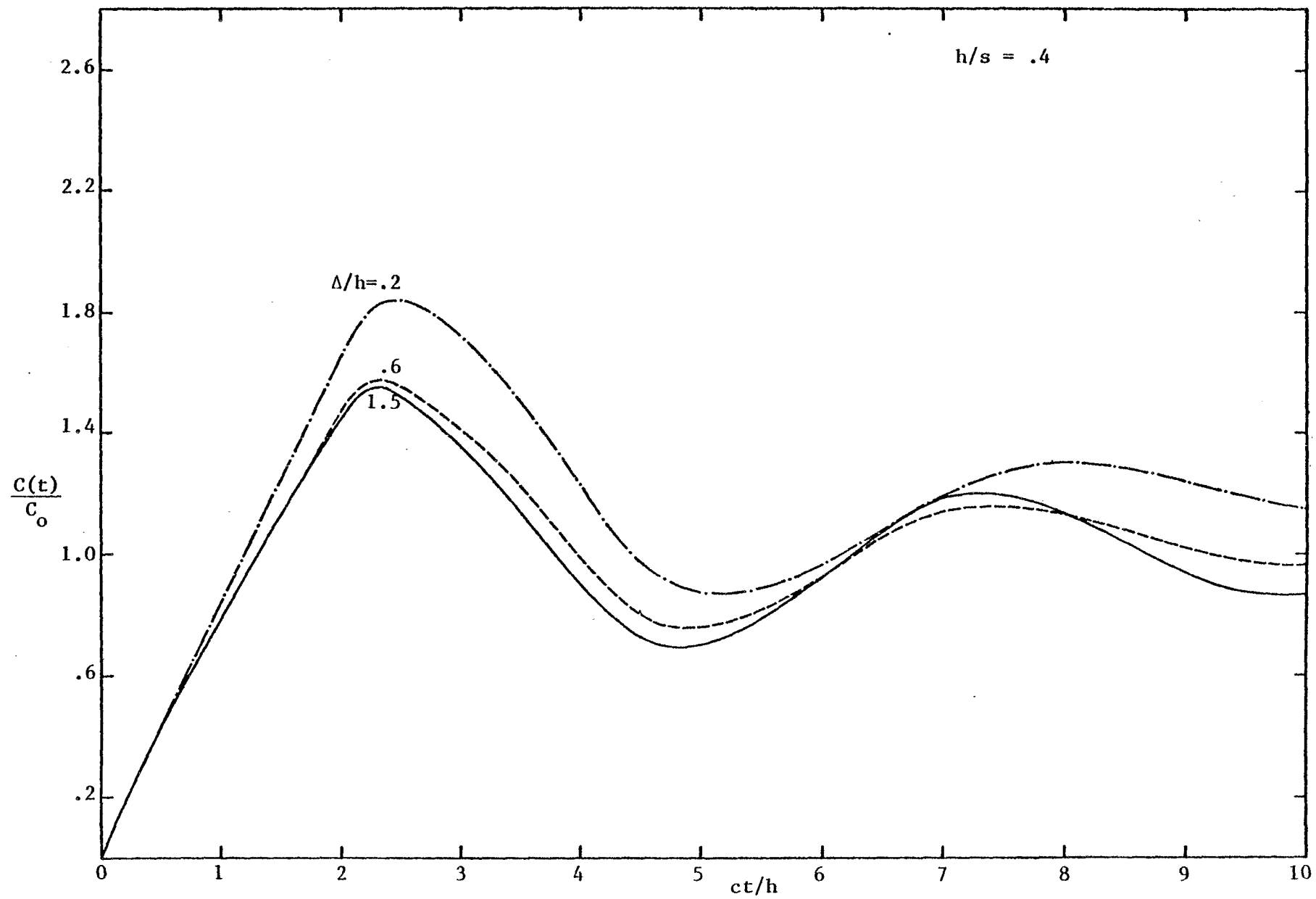
Figure 4c.   Time history of the total surface charge at the post's bottom end.
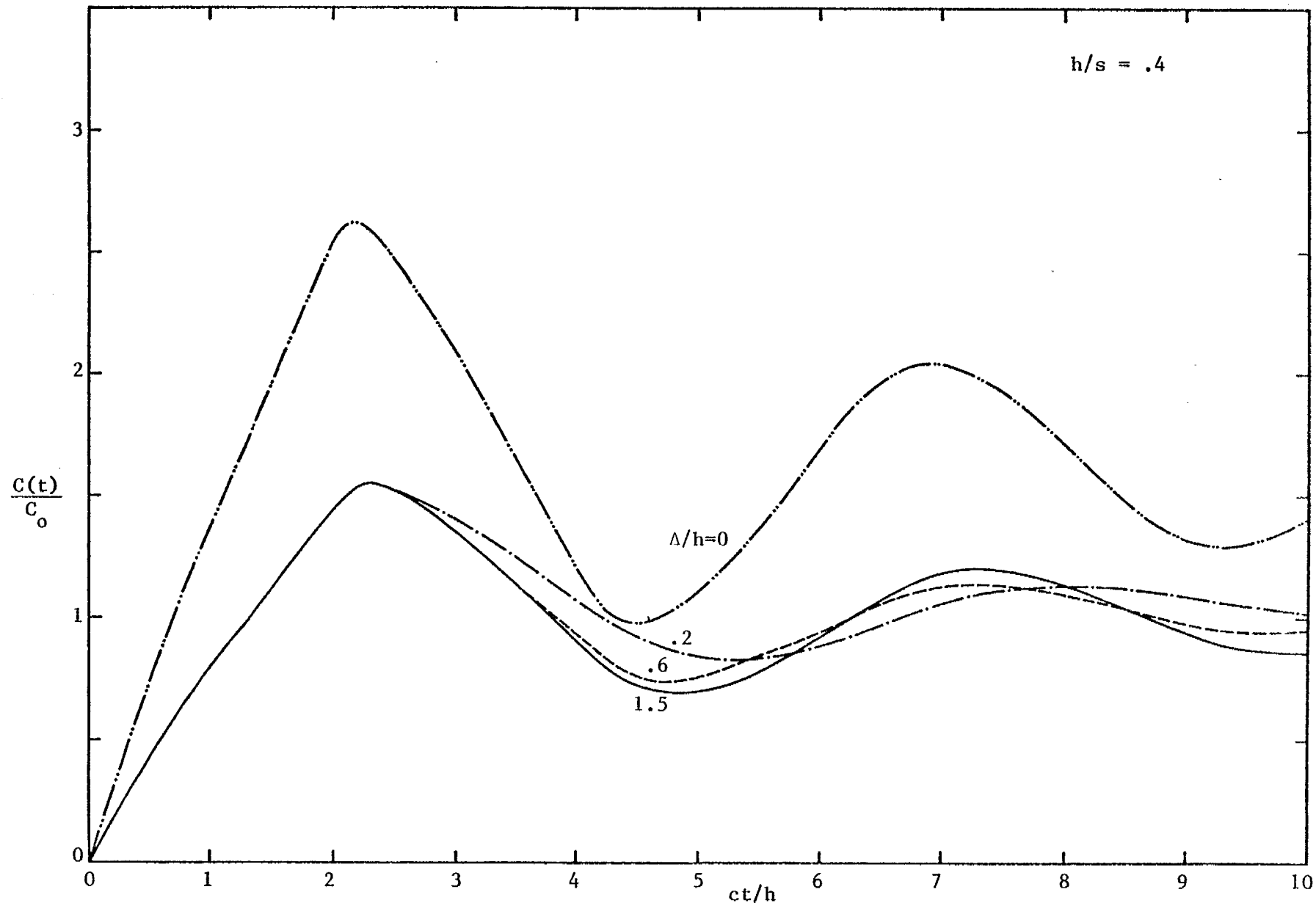
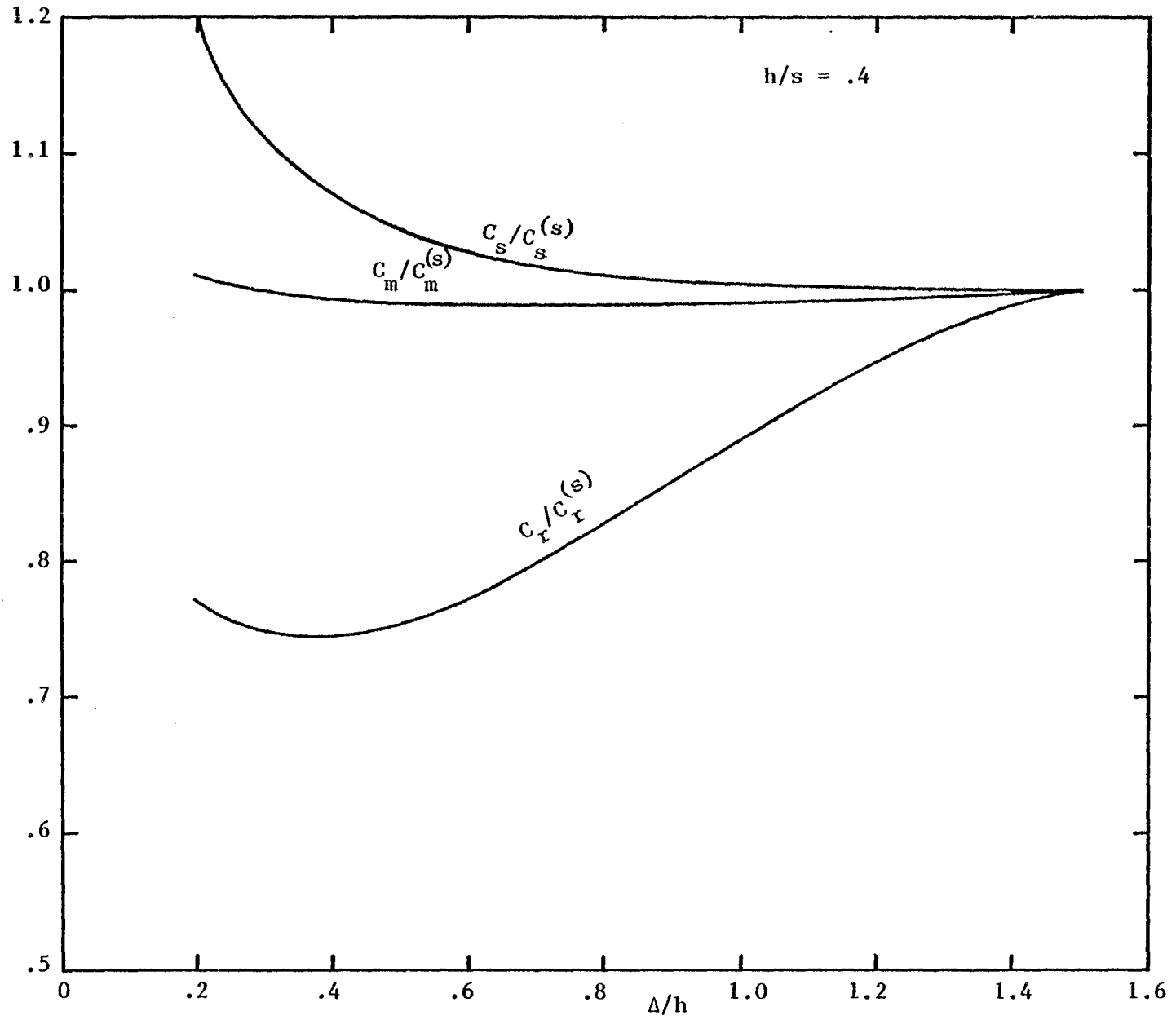Figure 4d. Time history of the total surface charge at the post's top end.

Figure 4e. Total surface charge at the post's bottom end versus Δ/h.

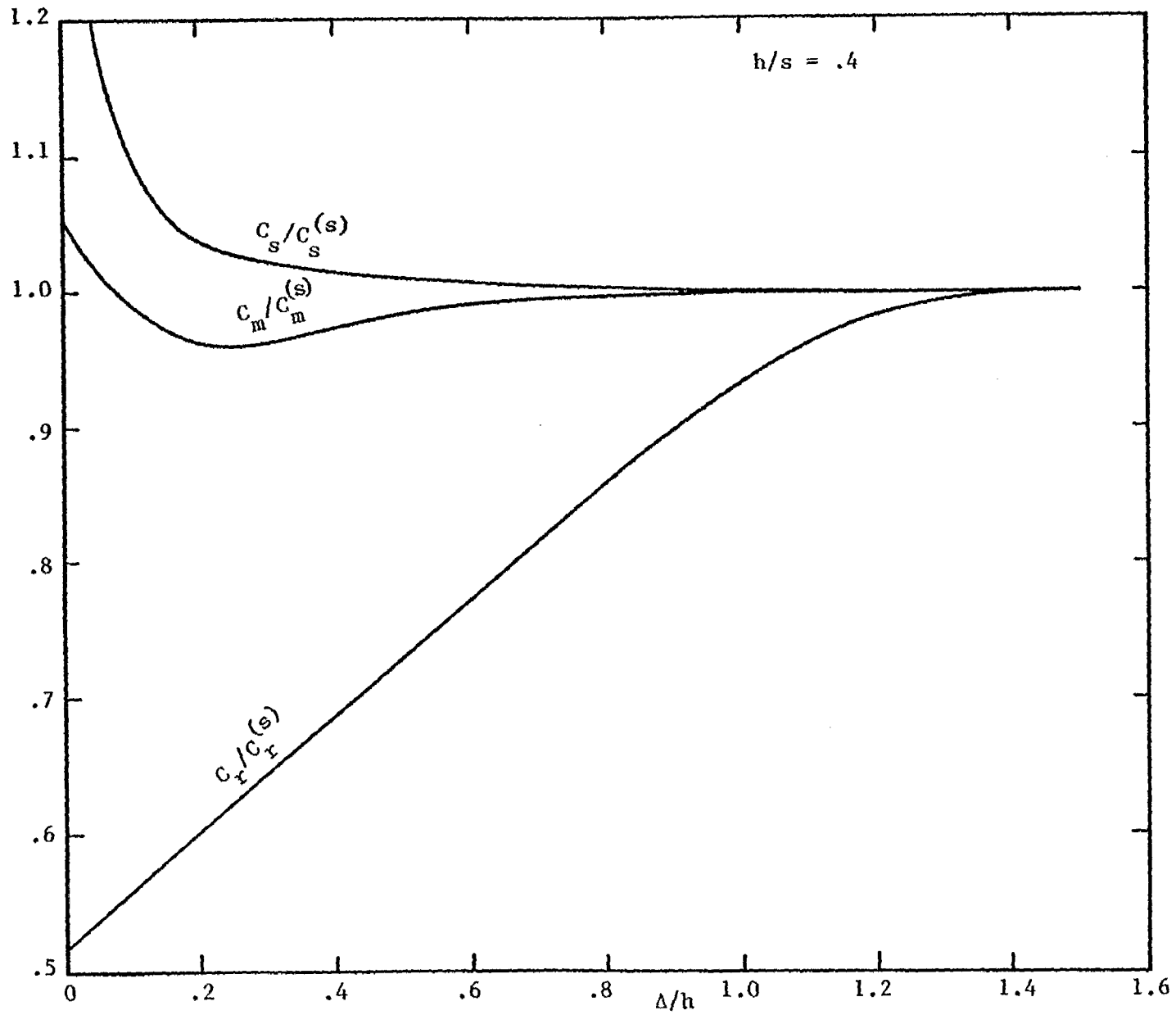Figure 4f. Total surface charge at the post's top end versus Δ/h.
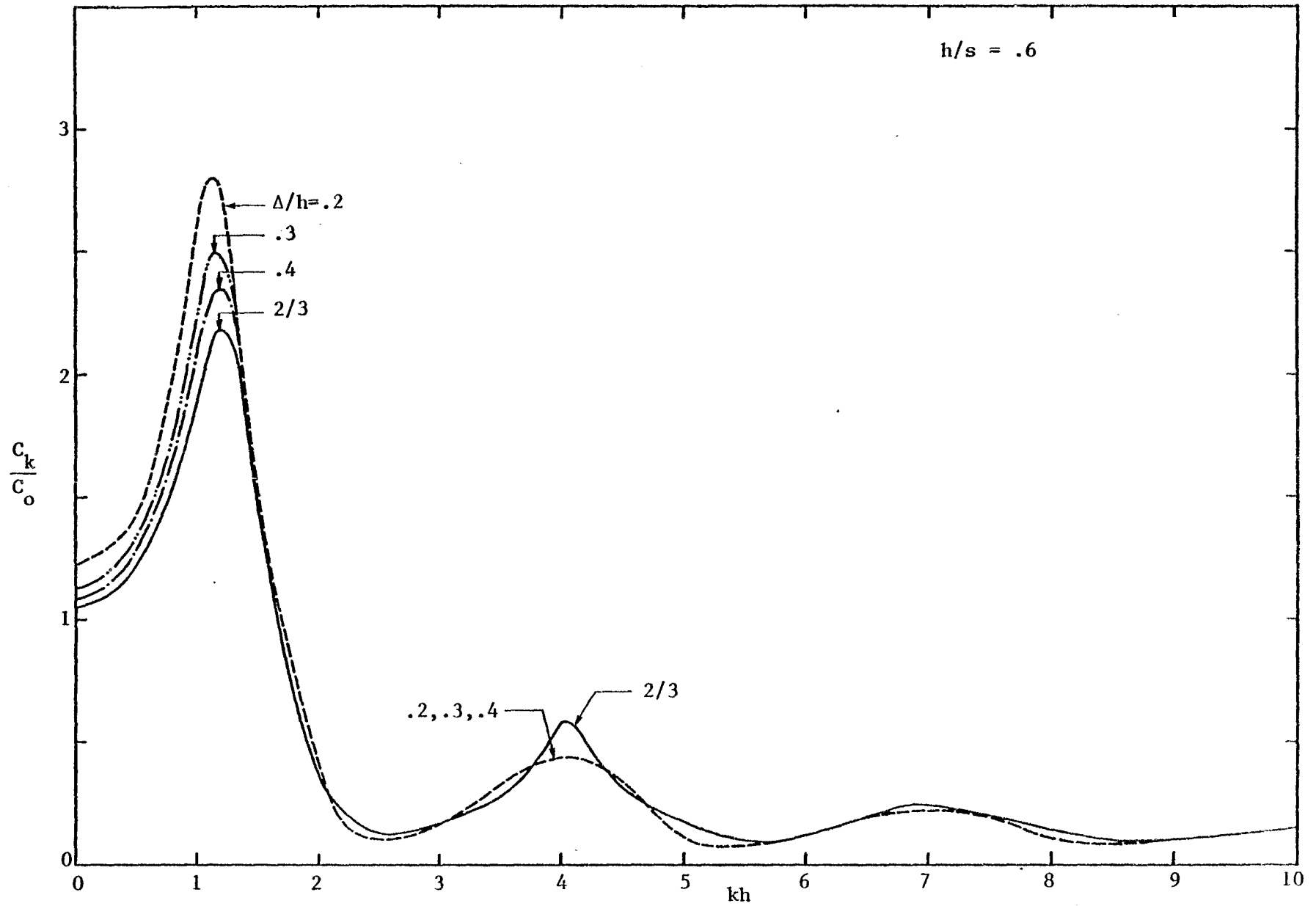
h/s = .6

Figure 5a. Frequency variation of total surface charge density at the post's bottom end.
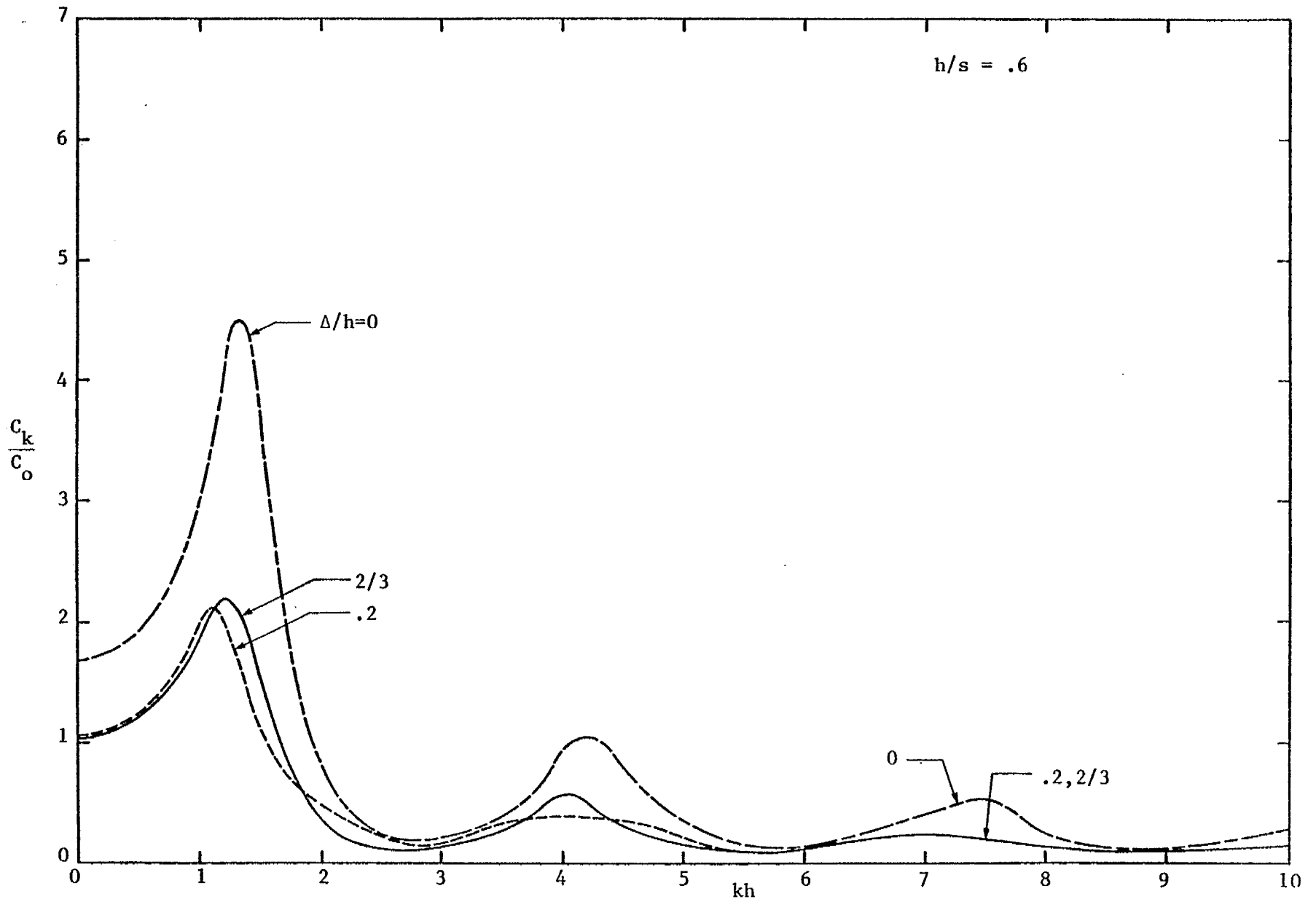
Figure 5b. Frequency variation of total surface charge density at the post's top end.
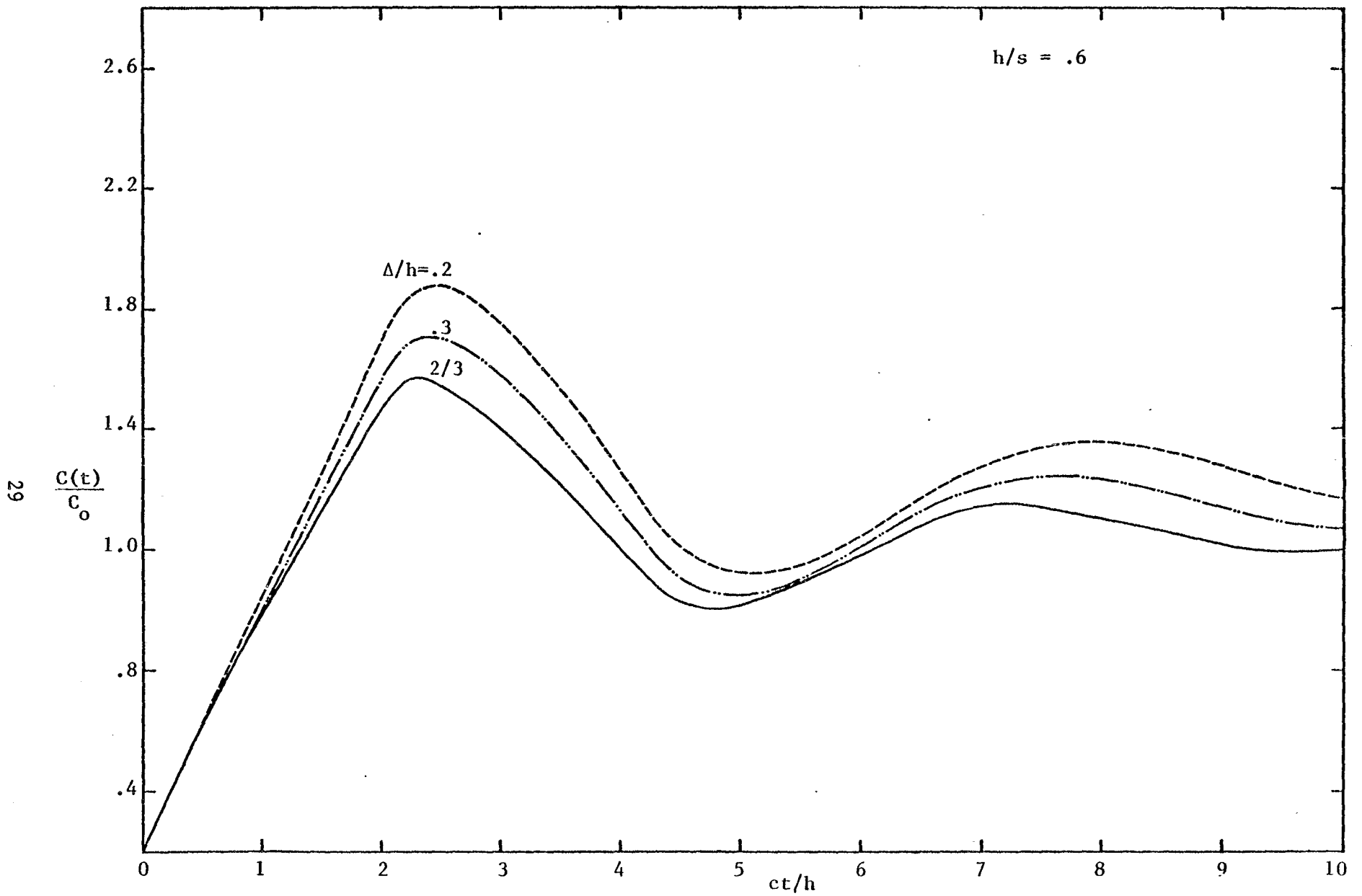
Figure 5c. Time history of the total surface charge at the post's bottom end.
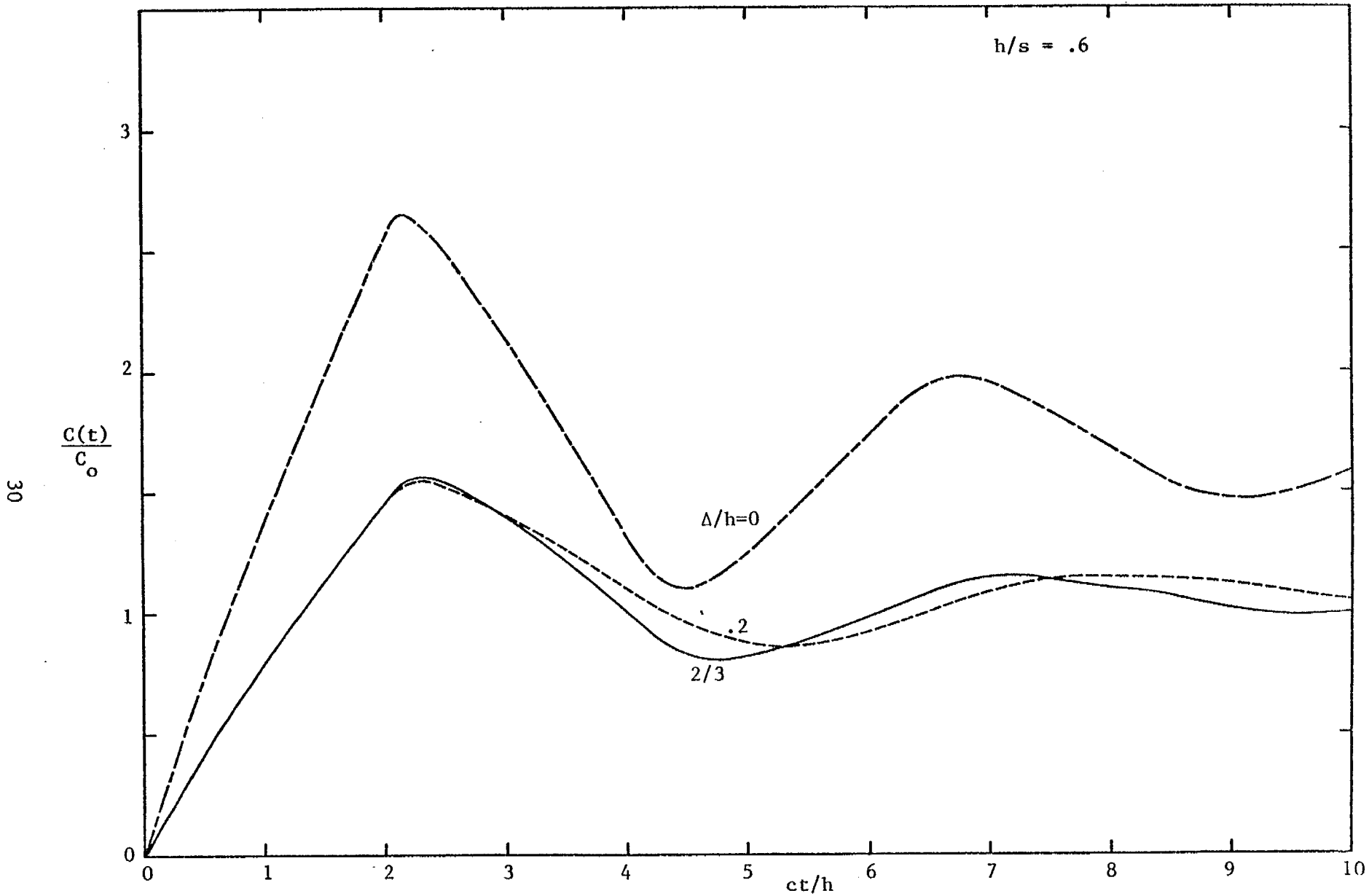
29

$$\frac{C(t)}{C_o}$$

h/s = .6

Δ/h=0

.2

2/3

ct/h

Figure 5d.   Time history of the total surface charge at the post's top end.
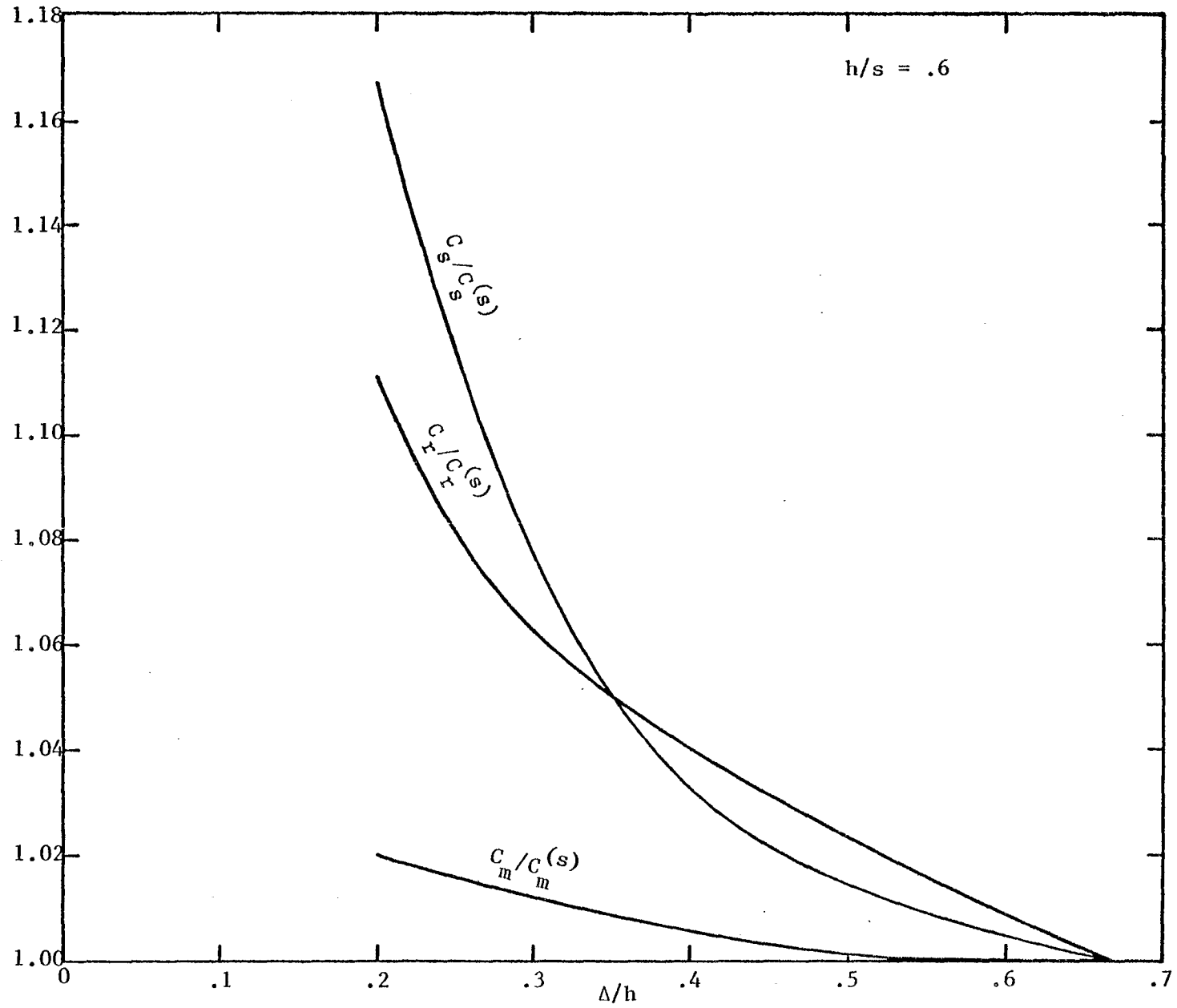
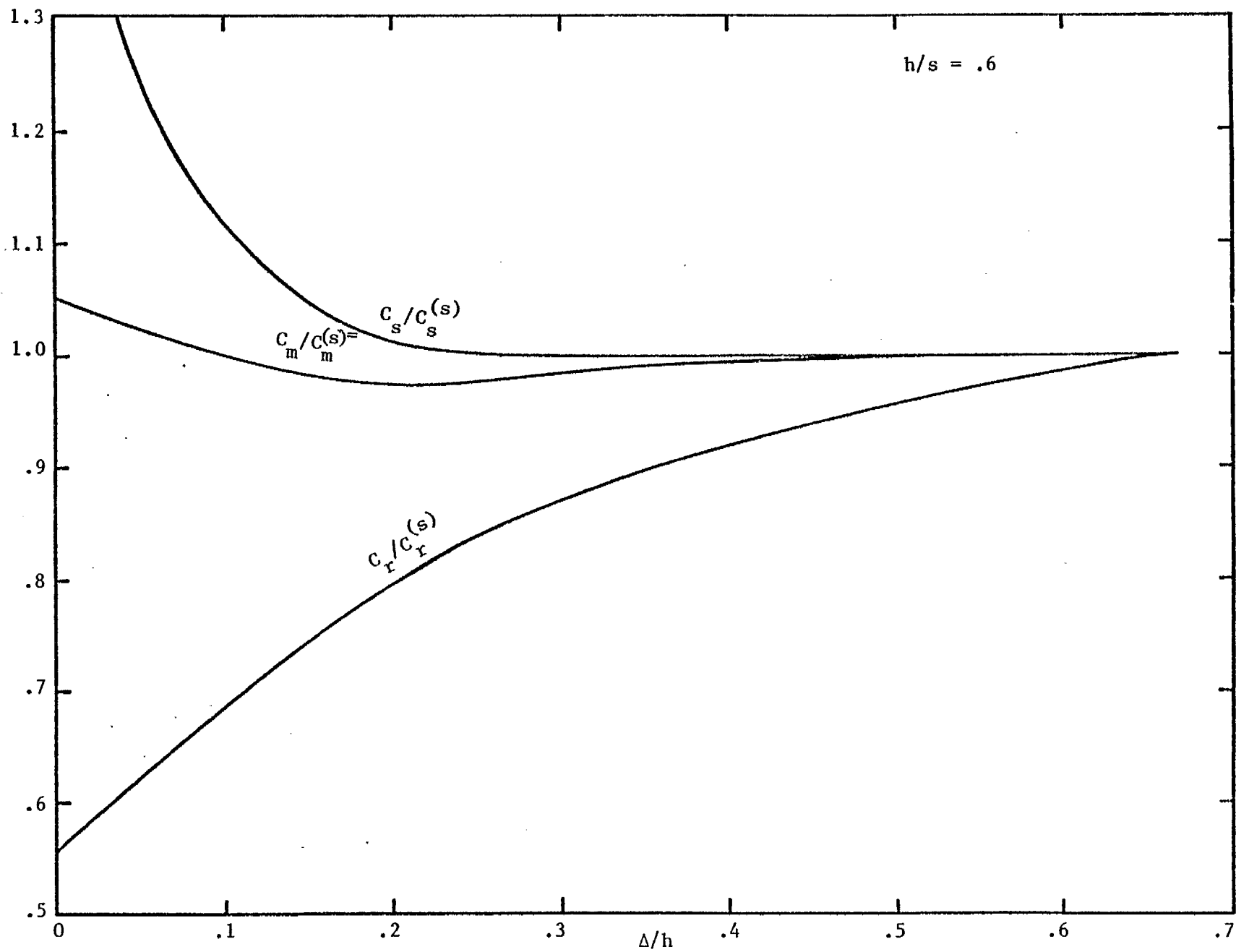Figure 5e.   Total surface charge at the post's bottom end versus Δ/h.

The graph shows three curves plotted against Δ/h (x-axis from 0 to .7) with values on the y-axis from .5 to 1.3. The label $h/s = .6$ appears in the upper right. Curves are labeled $C_s/C_s^{(s)}$, $C_m/C_m^{(s)} =$, and $C_r/C_r^{(s)}$.

Figure 5f.   Total surface charge at the post's top end versus Δ/h.

Acknowledgment

References

1. R. W. Latham and K. S. H. Lee, "Electromagnetic Interaction Between a Cylindrical Post and a Two-Parallel-Plate Simulator, I," Sensor and Simulation Note 111, July 1970.

2. K. S. H. Lee, "Electromagnetic Interaction Between a Cylindrical Post and a Two-Parallel-Plate Simulator, II (a Circular Hole in the Top Plate)," Sensor and Simulation Note 121, November 1970.

3. L. Marin, "A Cylindrical Post Above a Perfectly Conducting Plate, I (Static Case)," Sensor and Simulation Note 134, July 1971.

4. L. Marin, "A Cylindrical Post Above a Perfectly Conducting Plate, II (Dynamic Case)," Sensor and Simulation Note 136, August 1971.